Temperature dependant structural changes in thin films of random semifluorinated PMMA copolymers

Dieter Jehnichen,[1,a)] Peter Friedel,[1] Romy Selinger,[1] Andreas Korwitz,[1] Martin Wengenmayr,[2] Andreas Berndt,[1] and Doris Pospiech[1]

[1]*Leibniz-Institut für Polymerforschung Dresden e.V., Hohe Str. 6, D-01069 Dresden, Germany*
[2]*Technische Universität Chemnitz, Straße der Nationen 62, D-09111 Chemnitz, Germany*

Semifluorinated (SF) side chain polymers show phase separation between polymer backbone and SF side chains. Due to strong interaction between SF segments the side chains determine the structure behaviour strongly, often resulting in layered structures in which backbones and layers of SF side chains alternate. The interest in this work was directed to find out the dependence of these structures on concentration of SF side chains. Thin films of random copolymers consisting of methylmethacrylate (MMA) and semifluorinated side chain methacrylate (SFMA) segments and with different fluorine content in the perfluoroalkyl side chains (abbreviated as H10F10 and H2F8) were prepared by spin-coating. Phase separation and structure changes were initiated by external subsequent annealing. Corresponding bulk material served as basic information. Generation of ordered structures and variation of film parameters were observed using different X-ray scattering methods (XRR, GIWAXS, and GISAXS). The phase behaviour in bulk is governed by the SF side chain amount and their specific fluorine content which control the self-organization tendency of SF side chains. Additionally, the confinement in thin films generates an orientation of side chains normally to film surface.

Key words: T-dependant X-ray scattering, GISAXS, phase separation, thin films, random copolymers, semifluorinated polymers

a) Author to whom correspondence should be addressed. Electronic mail: djeh@ipfdd.de

 0885-7156/2013/28(S2)/S2/1/$18.00 ©2013 JCPDS-ICDD

https://doi.org/10.1017/S0885715613001073 Published online by Cambridge University Press

I. INTRODUCTION

Semifluorinated (SF) side chain polymers show a structure behaviour which is characterized by phase separation between polymer backbone and SF side chains (e.g., Höpken and Möller, 1992; Wang *et al.*, 1997), driven by huge Flory-Huggins interaction parameters. As a result of the strong interaction between the fluorinated segments, e.g. perfluoroalkyl groups, the side chains determine the structure behaviour strongly (Friedel *et al.*, 2000; Gottwald *et al.*, 2002) and influence physical parameters and application properties significantly (Gopalan *et al.*, 2002; Appelhans *et al.*, 2005; Tsuwi *et al.*, 2007). In general, sufficiently long SF side chains are organized in ordered structures (Li *et al.*, 2002; Busch *et al.*, 2007). The internal microphase separation leads mostly to smectic layered structures in which the backbones and layers of SF side chains alternate (Jehnichen *et al.*, 2001; Pospiech *et al.*, 2003b). Former experiments examined in detail the behaviour of different polymers with H10F10 side chains [-O-$(CH_2)_{10}$-$(CF_2)_{10}$-F] (Pospiech *et al.*, 2001; Pospiech *et al.*, 2003a). Combination of different scattering methods and thermal treatments yielded in understanding the special side chain structure characterized by interdigitation and tilt of side chains (Jehnichen *et al.*, 2004; Jehnichen *et al.*, 2007). Incorporation of H10F10 side chains lead in all types of polymer backbones used (aromatic and aliphatic polyesters, polysulfones, polypropylene copolymers) to distinguished phase separation with layered structures having similar *d*-spacings (Jehnichen *et al.*, 2007; Jehnichen *et al.*, 2011). Additionally, such structures gave rise to unusually low surface free energies (Wang *et al.*, 1997; Grundke *et al.*, 2001; Pospiech *et al.*, 2003b; Galli *et al.*, 2005) due to the formation of a similar structure in the surface region attended by enrichment of F-containing segments in that layer (Pospiech *et al.*, 2003c).

The interest in this work was directed to find out the dependence of the structure behaviour on the fluorine concentration and side chain length. Random copolymers consisting of methylmethacrylate (MMA) and semifluorinated side chain methacrylate (SFMA) segments were synthesized by radical polymerization varying the structure of the side chain: H10F10 and H2F8 [-O-$(CH_2)_2$-$(CF_2)_8$-F] (Figure 1 and Table I). Thin films with roughly comparable films thicknesses were prepared by spin-coating.

https://doi.org/10.1017/S0885715613001073 Published online by Cambridge University Press

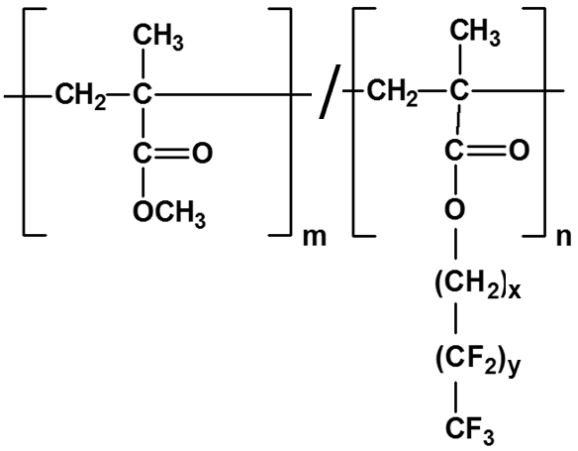


Figure 1: Chemical formula of random P(MMA/SFMA-HxFy+1) copolymers with (x,y) = (2,7) and (10,9) under investigation.

TABLE I. Sample overview.

Sample	Sample form	SF side chain	SF concentration (mol%)	Molar mass M_w (g/mol)
H2F8-41	bulk	H2F8	41	18.100
H2F8-71	bulk	H2F8	71	5.000
H10F10-38	bulk	H10F10	38	22.000
H10F10-66	bulk	H10F10	66	6.700
H2F8-37	film	H2F8	37	64.000
H2F8-72	film	H2F8	72	5.900
H10F10-36	film	H10F10	36	27.600
H10F10-54	film	H10F10	54	19.000

The phase separation and its changes were initiated by external subsequent annealing of thin films (different procedures). Appropriate temperature steps were determined investigating the corresponding bulk material via combined T-SAXS / T-WAXS showing characteristic phase transition temperatures. Generation of ordered structures and variation of film parameters were observed using different X-ray scattering methods (XRR, GIWAXS and GISAXS).

https://doi.org/10.1017/S0885715613001073 Published online by Cambridge University Press

II. EXPERIMENTAL

A. Sample preparation

1. Synthesis

Random P(MMA/SFMA) copolymers were synthesized by radical polymerization in bis(trifluoromethyl)benzene (BFMB). Therefore, destabilized monomers, solvent BFMB and initiator azobis(isobutyro)nitrile (AIBN) were filled into a dried Schlenk flask. It was purged and deoxygenated by three freeze-thaw cycles. The flask was placed into a heating bath at 80 °C for polymerization under stirring for 4 h. The flask was cooled down to room temperature and then a mixture of BFMB and chloroform (1/1 v/v) was added to dilute the solution. The solution was precipitated into methanol, filtered off and dried in vacuum at 50 °C for 12 h to obtain a white solid. Relative averaged molar masses M_w and M_n were determined by size-exclusion chromatography (SEC) yielding values relative to narrow distributed PMMA standards.

2. Film preparation

Thin polymer films were prepared by spin-coating (2000 rpm / 30 s) of 2 wt% filtered (through 0.45 µm Teflon filter) polymer solution in BFMB onto pre-cleaned silicon wafers. The films were dried at 30 °C for 24 h in vacuum. For XRR and GIWAXS experiments, off-line annealing (in subsequent steps up to 160 °C considering transition temperatures of the copolymers) was performed, followed by a fast cooling to room temperature.

B. X-ray scattering experiments

1. T-SAXS / T-WAXS

Combined temperature-dependant small- and wide-angle X-ray scattering (T-SAXS / T-WAXS) in transmission geometry were carried out at the Soft Condensed Matter Beamline A2 (HASYLAB @ DESY Hamburg, λ_{A2} = 0.15 nm) applying linear detectors (both mounted perpendicular to the primary beam, detector channels correspond to the scattering vector with different offsets concerning SAXS and WAXS detector). Oven experiments were executed by heating/cooling rates of 3 K/min or by fast cooling.

https://doi.org/10.1017/S0885715613001073 Published online by Cambridge University Press

2. XRR and GIWAXS

X-ray reflectometry (XRR) was carried out at diffractometer XRD T/T (GE Inspection Technologies Ahrensburg, Germany) in symmetric step-scan mode with $\Delta 2\Theta$ = 0.01° and t = 3 s (Cu $K\alpha$ radiation). Grazing incidence wide-angle X-ray scattering (GIWAXS) was carried out at the same diffractometer XRD T/T in asymmetric step-scan mode with $\Delta 2\Theta$ = 0.05° and t = 20 s (Cu $K\alpha$ radiation) and grazing angle 0.7° (irradiated film area 10×15 mm^2). The layer distances (d-values) were calculated using Bragg's law onto the layer reflections (maximum positions in 2 Θ).

3. T-GISAXS

Temperature-dependant grazing incidence small-angle X-ray scattering (T-GISAXS) was carried out at the Beamline BW4 (HASYLAB @ DESY Hamburg, λ_{BW4} = 0.138 nm) applying the area detector MarCCD (Marresearch Inc., USA). 2D-pattern within incidence angles α_i (0.03° - 0.30°), close to the critical angles α_c (polymer film, e.g., pure PMMA: $\alpha_c \approx 0.146°$; substrate SiO_x: $\alpha_c \approx 0.20°$) were accumulated with sufficiently high measuring time to find an optimal α_i for oven experiments, which were executed by heating/cooling rates of 3 K/min or by fast cooling.

III. RESULTS AND DISCUSSION

A. Bulk behaviour

Figures 2 and 3 illustrate the temperature-dependant scattering behaviour of the bulk material **H10F10-38** starting from the as-synthesized state. This state is characterized as powder-like particles that precipitate from synthesis. The first heating run shows the formation to be seen at the spatial separation of the chemically incompatible segments and improvement of the phase morphology as seen as appearance of well-shaped reflections. At temperatures higher than T_m (side chain melting) and lower than T_i (isotropization), a typical smectic layer structure (see Figure 2) with negative coefficient of linear expansion of the layer distance (1st and 2nd order reflection of the side chain layers changing going from d ~ 4.7 nm to 4.2 nm) was found. This behaviour resembles that of semifluorinated polyesters (Jehnichen *et al.*, 2004 and 2007). At T_i the layer structure is lost. Only an "amorphous-like" broad maximum is visible until 150 °C, which is above the glass transition temperature T_g of the base main chain PMMA. The fluorinated part of the SF side

https://doi.org/10.1017/S0885715613001073 Published online by Cambridge University Press

chains are comparable to hexagonally packed PTFE chains in helix conformation. In the corresponding WAXS pattern (see Figure 3) this lateral arrangement disappears above T_m ~ 57 °C and is re-generated in the cooling cycle below T_m. For T > T_m, only a broad amorphous scattering maximum remains.

Copolymers with H2F8 side chains show a much weaker pronounced layer formation with a *d*-value of ~3.0 nm corresponding to the shorter side chain. Smectic layers as well as lateral correlation between the side chains could not be observed. This was expected due to the shorter SF segment of the side chain. This result is valid for both low and high SF comonomer concentrations. For both side chain types, the lateral correlation effects are significantly lower in comparison to the corresponding diblock copolymers having comparable SF concentration (Jehnichen *et al.*, 2011). All bulk data are summarized in Table II.

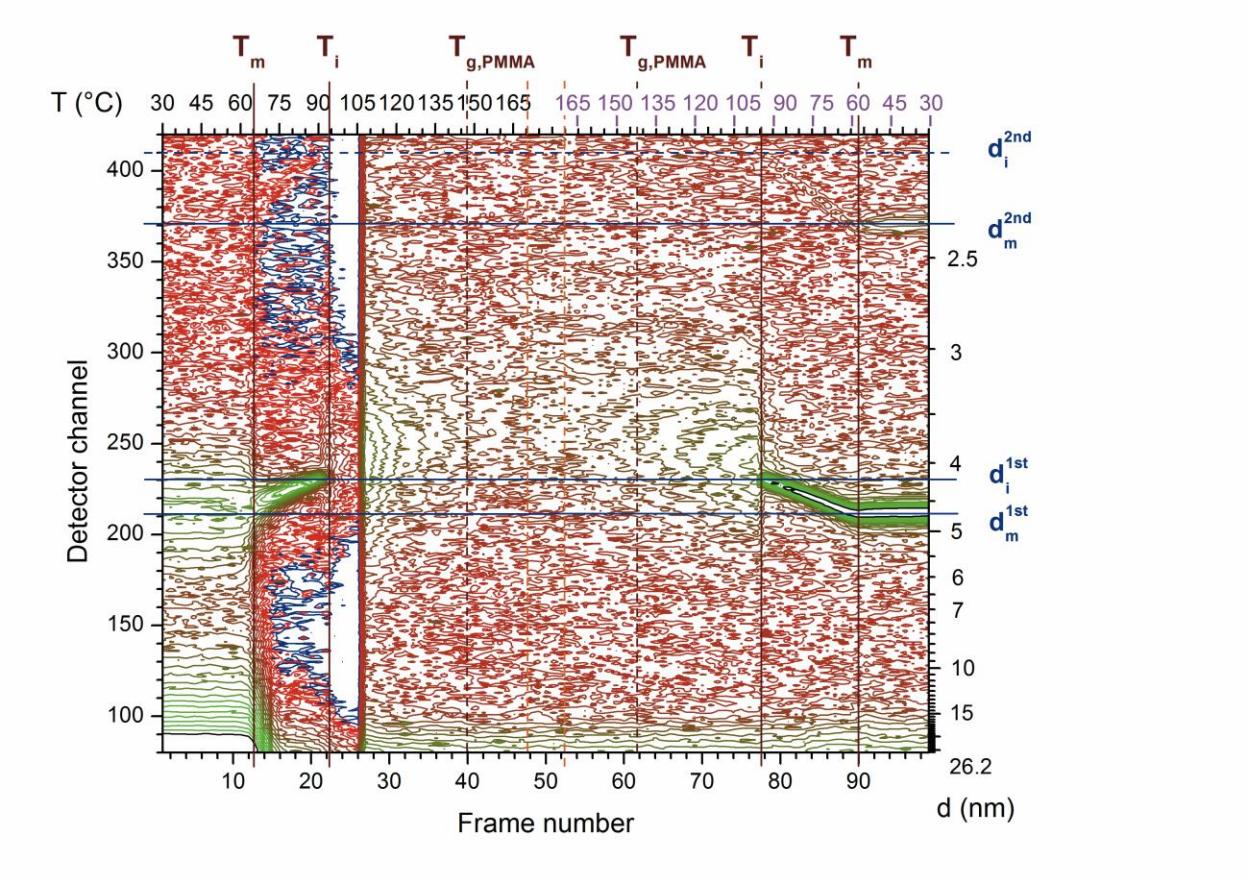


Figure 2: (Colour online) T-SAXS - Contour plot of sample **H10F10-38** (as-synthesized). Scattering intensity plot (false colour representation) log(*I*) vs. *T* and vs. *d*.

https://doi.org/10.1017/S0885715613001073 Published online by Cambridge University Press

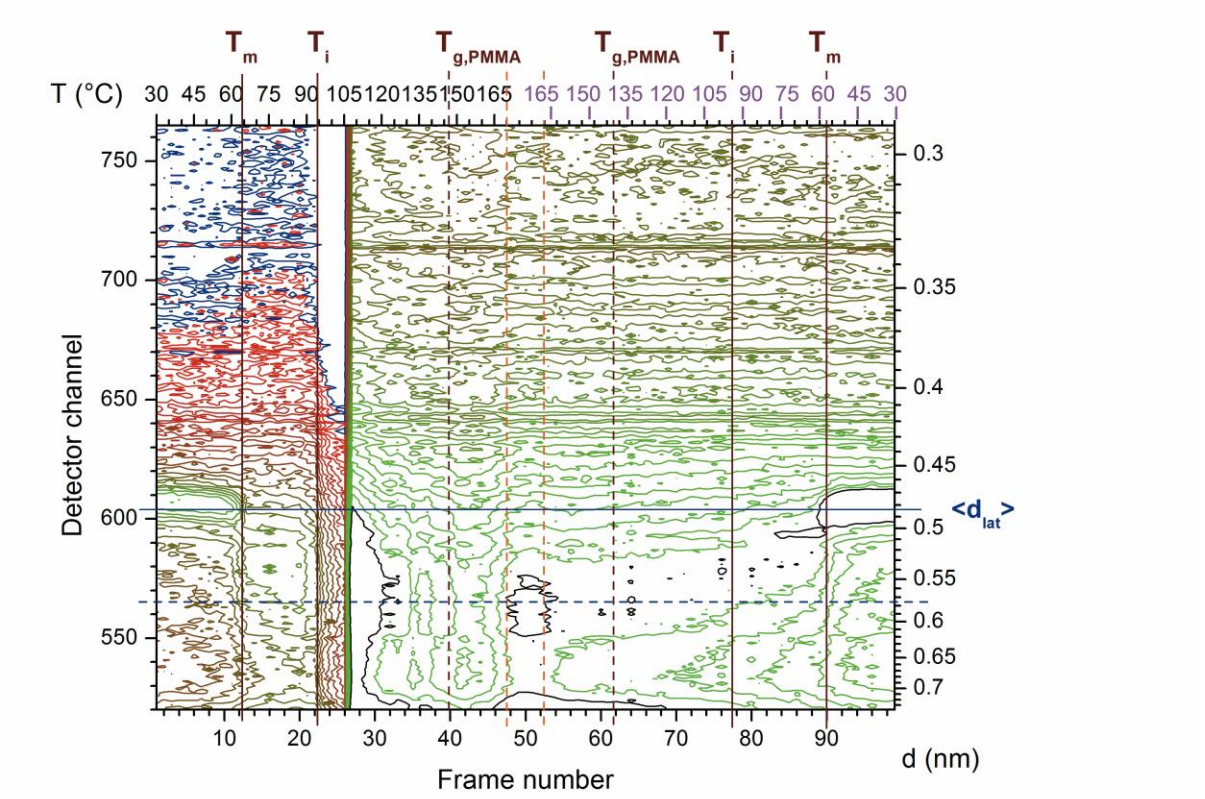


Figure 3: (Colour online) T-WAXS - Contour plot of sample **H10F10-38** (as-synthesized). Scattering intensity plot (false colour representation) log(*I*) vs. *T* and vs. *d*.

TABLE II. Results of *T*-dependant scattering experiments of the investigated samples (bulk parameters from 1st cooling run).

	Sample	**H2F8-41**	**H2F8-71**	**H10F10-38**	**H10F10-66**
T (°C)		**T-SAXS**			
95	Layer distance	--	--	4.18	4.05
30	*d* (nm)	3.0	2.8	4.65	4.70
		T-WAXS			
30	Mean chain distance $<d_{lat}>$ (nm)	0.520	0.525	0.485	0.490

B. Thin films

1. XRR and GIWAXS

As-prepared films (film thicknesses from 74 to 90 nm) show very low roughness and good preparation reproducibility. The as-prepared films were stepwise annealed and after fast quenching offline examined by XRR. In the temperature range of T_m the generation of the layered structure shows a different behaviour dependant on the side chain type and

https://doi.org/10.1017/S0885715613001073 Published online by Cambridge University Press

concentration. In the case of H10F10 side chains (Figure 4 for lower H10F10 concentration), the layer arrangement starts as in the bulk at $T_m < T < T_i$. The layer distance (found for the second annealing step 80 °C) is 4.2 nm (about 0.4 nm smaller compared to the bulk value after complete heating/cooling cycle). For higher annealing temperatures (up to T = 160 °C) more or less frozen states were found accompanied by degradation of the film which was deduced from the higher roughness. In principle, this is confirmed by films having higher H10F10 concentration, but much lower film thicknesses (14 nm). Certainly, the discussion of details with respect to this is difficult due to the restricted film thickness (only ~3 layers can be formed by phase separation: the lower one in interaction to the silica substrate, the upper one in interaction with air).

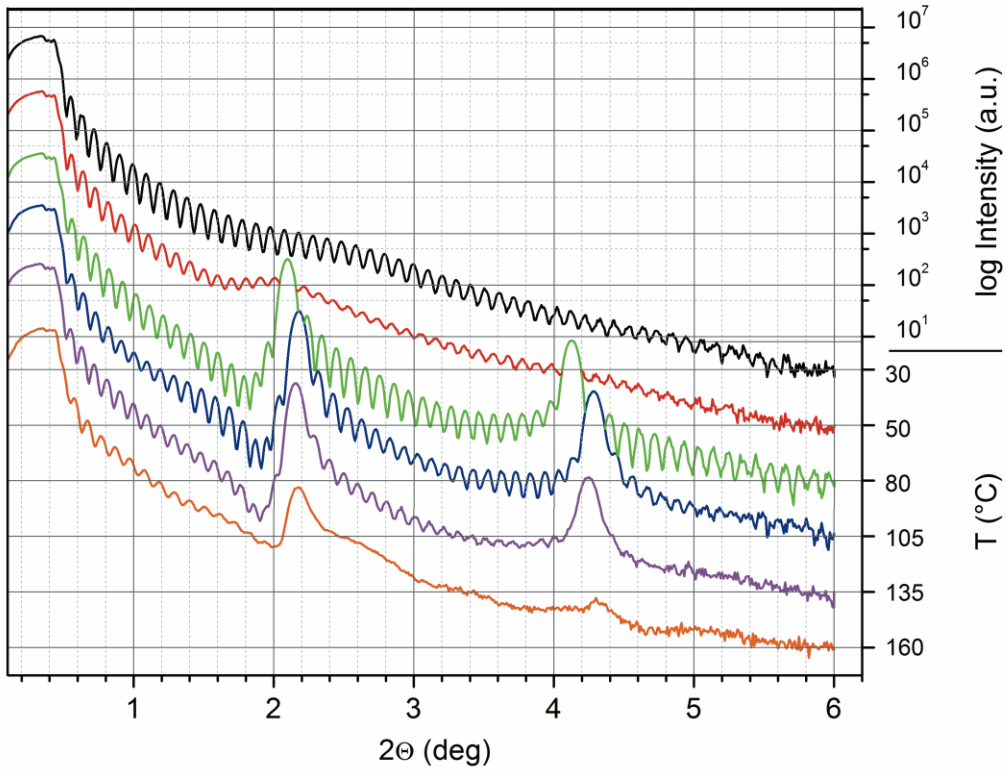


Figure 4: (Colour online) XRR curves of sample **H10F10-36** (at room temperature) after subsequent annealing (measured after quenching to room temperature).

https://doi.org/10.1017/S0885715613001073 Published online by Cambridge University Press

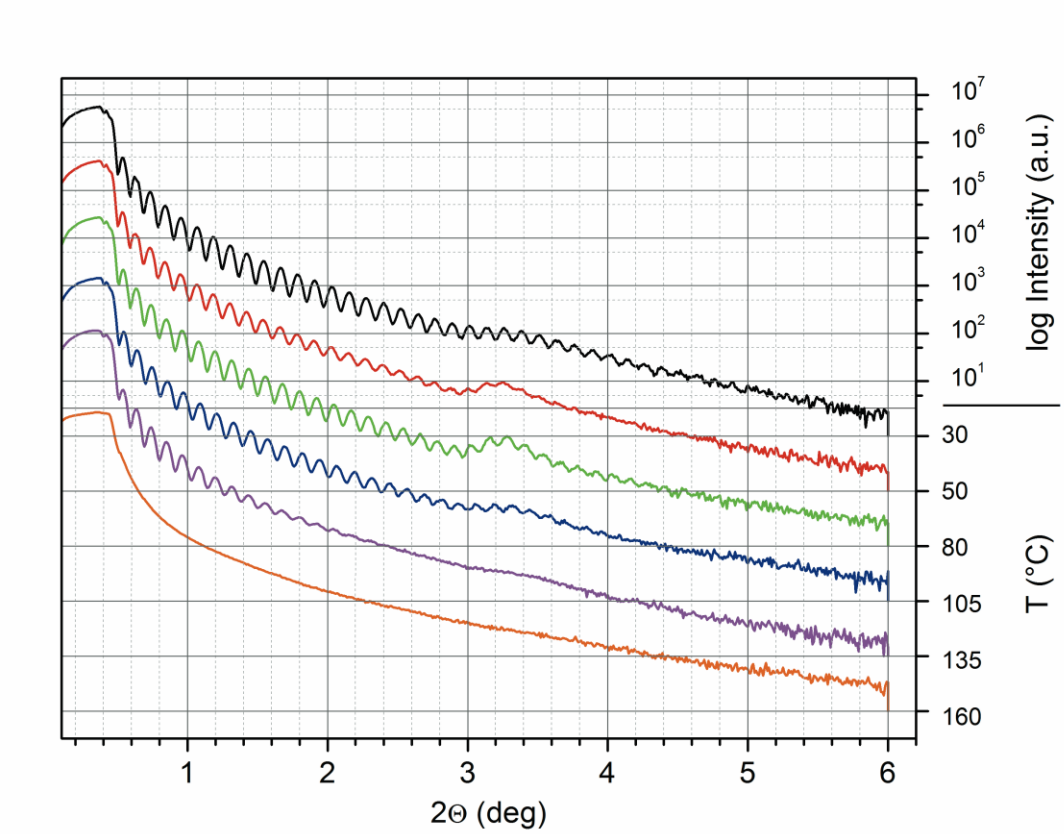


Figure 5: (Colour online) XRR curves of sample **H2F8-72** (at room temperature) after subsequent annealing (measured after quenching to room temperature).

Inspired by an obvious model based on both chemical structure and compatibility behaviour of the different segments (Figure 6), a simple model which is characterised as a stack of repeating sublayers was chosen to fit the experimental XRR curves. As a preliminarily result was found a stack of 20 repeating units verifying the Bragg reflection with d = 4.28 nm and internal substructure of a PMMA-like sublayer with d_{mch} = 2.70 nm (representing the main chain and a part of the alkyl segment of the side chain) and a PTFE-like sublayer with d_{sch} = 1.58 nm (representing mainly the perfluorinated part of the side chain). The ratio d_{mch} to d_{sch} is in line with the assumed model and the spatial parameters fit well the film thickness of 85.6 nm. The adapted electron densities in the respective sublayer are reduced by about 10 % in relation to the bulk parameters of PMMA and PTFE, respectively. The discussed numerical values are valid for the XRR curve of sample **H10F10-36** measured after annealing with 80 °C (compare Figure 4).

https://doi.org/10.1017/S0885715613001073 Published online by Cambridge University Press

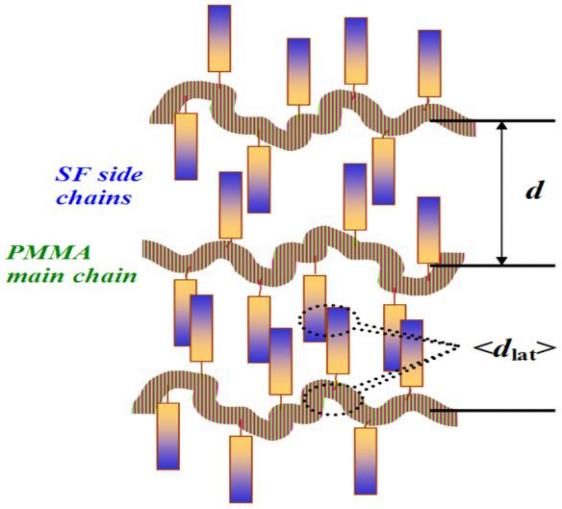


Figure 6: (Colour online) Schematically simplified structure of P(MMA/SFMA) copolymers with well-ordered layers.

As expected from the bulk results, H2F8 copolymer films show a different behaviour (Figure 5). In the case of lower H2F8 concentration no layers are generated during the annealing process. Only a very weak and broad scattering maximum occurs at the position where the Bragg maximum would be expected. At temperatures higher than T_g of the main chain the film parameters reflect thermal degradation showed by increasing roughness. The layer arrangement in films from copolymers with higher concentration starts at T ~ 50 °C. The layer generation is significantly stronger compared to the bulk and appears at lower temperatures. But, the stability of the layered structure at higher annealing temperatures is lower (which can also be influenced by the quenching process from melt). The layer distance d was estimated to be ~2.8 nm (from Bragg maximum) and is about 0.3 nm lower as in the bulk.

The GIWAXS experiment exhibits a broad scattering maximum corresponding to superimposed scattering parts from non-ordered main chains PMMA and the not well-ordered SF side chains in pseudo-hexagonal packing. Thus, this maximum corresponds to an intermolecular distance which represents basically a "mean chain distance" $<d_{lat}>$ considering the main chains, the side chains and their arrangements to each other (compare Figure 6). For copolymers with H10F10 side chains the maximum corresponds stronger to a distance $<d_{lat}>$ comparable to poly(tetrafluoro ethylene) chains in well-crystallized PTFE homopolymer ($<d_{lat}> \approx d_{hex(100)}$ = 0.489 nm). The tendency to generate a pseudo-crystalline order (as found in bulk experiments) is significantly reduced in thin films. There was also no improvement by annealing. In samples with H2F8 side chains (i.e., shorter side chain and lower F content) this small ordering effect is

https://doi.org/10.1017/S0885715613001073 Published online by Cambridge University Press

much lower. Thus, the distance $<d_{lat}>$ is smaller and rather similar to that of PMMA. All data $<d_{lat}>$ experimentally found by T-GIWAXS are listed in Table III and those fond by T-WAXS in Table II yet. Due to the orientation of the layer structure and the arrangement of the side chains nearly perpendicular to the substrate (see discussion of GISAXS, below) the GIWAXS intensity caused by these structures is decreased additionally.

2. T-GISAXS

The technique of grazing incidence small-angle X-ray scattering (GISAXS) was successfully applied to soft condensed matter samples in the thin-film geometry since several years (Rauscher *et al.*, 1995; Müller-Buschbaum, 2009). Nanostructures parallel and perpendicular to the sample surface are observable in thin diblock copolymer or other micro-phase separated polymer based films (Müller-Buschbaum, 2003; Busch *et al.*, 2006). The basic ideas and possibilities of the GISAXS technique are illustrated in Figures 7a and b.

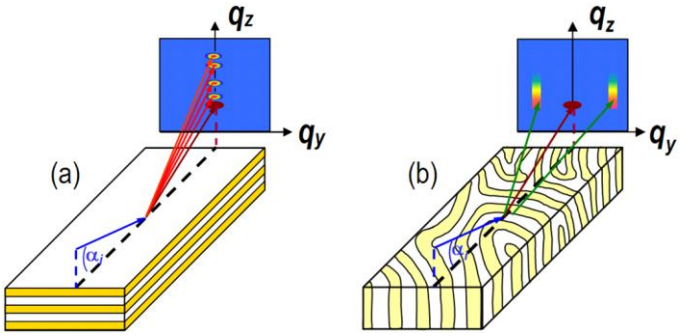


Figure 7: (Colour online) Schematic drawing of scattering geometries for illustration of GISAXS experiments of a thin film structure with lying layers ((a) - parallel to substrate; sample in *x*,*y* plane and scattering plane defined by *x*,*z* plane) and standing layered structures ((b) – perpendicular to the substrate). The intensity trace on the blue screen in (a) (detector: *y*,*z* plane) corresponds to the detector scan (in-plane scan) $I = I(q_z)$ (vertical slices, $q_y = 0$), which basically probes structures perpendicular to the sample surface. The intensity trace on the blue screen in (b) corresponds to the out-of-plane scan $I = I(q_y)$ (horizontal slices, e.g. $q_z = q_{cr}$, conform to the critical angle α_{cr} of one copolymer component), which basically probes lateral structures in the sample surface. The corresponding *d*-values of the scattering maxima (correlation peaks) in the intensity scans reflect spatial structure parameters as projection onto the scattering vector direction. The specular reflected beam ($\alpha_i = \alpha_f$) was shielded by a beam stop, whereas the transmitted beam (close to the primary beam direction) was absorbed by the sample. The GISAXS pictograms were adapted from Busch (2003).

Figures 8 (a) to 8 (f) depict the *T*-dependant scattering behaviour of the 89 nm thin film consisting of **H10F10-36** as example for the polymer films under investigation. The chosen detector area of the GISAXS pattern contains the direct beam position (lower edge) and cover the scattering area for lateral *d*-values > 3.9 nm and normal *d*-values > 2.8 nm.

https://doi.org/10.1017/S0885715613001073 Published online by Cambridge University Press

The as-prepared sample state (room temperature) shows weak lateral correlation peaks at 4.72 nm and a broad halo in the detector scan. During heating the lateral peaks disappear and for T > 84 °C a strong Bragg reflection at 4.69 nm is generated in the detector scan. This reflection shows a marked sickle-like azimuthal intensity distribution proving the unidirectional orientation of the layers parallel to the substrate (lying layers) as well as narrow deviation behaviour. The formerly standing layers are newly oriented. Following this model, the existence of nearly perpendicularly standing SF side chains can be concluded. Additionally, a second scattering maximum occurs at higher scattering angles which cannot be understood by usual application of Bragg's law. Different scenarios may be discussed: (a) The second scattering maximum could be caused by multiple reflection effects in the film morphology, too. So it can be imagined to get reflections from the film surface directly as well also from the interface to the silicon substrate. In films with excellent geometric parameters versus the irradiated area a standing wave field cannot be excluded. To clarify this reflectivity behaviour, GISAXS experiments should be performed at different film thicknesses in dependence on both T and incident angle α_i in detail, which has to be varied from $\alpha_i < \alpha_c$ to $\alpha_i > \alpha_c$ and considering the fluorine content of the film material. These measurements were not possible in the frame of the work discussed here. (b) As suggested by T-SAXS, two different layer structures could be coexistent in a distinct temperature range between room temperature and isotropization temperature (RT … T_m ... T_i), if it can be assumed that the smectic layer structures with d-values between 4.2 and 4.7 nm are frozen or hindered to relax. (c) Furthermore, another possibility to describe this phenomenon is to treat it in a similar manner like diffraction of random copolyesters (Mitchell and Windle, 1985). It is imaginable that the polymer chains stand like brushes on the substrate with liquid-like lateral correlation to each other. Secondly, the polymer chains P(MMA/SFMA) have random distribution of the comonomers MMA and SFMA and thus fill out the film thickness completely. A model of randomly distributed chains is able to cause diffraction patterns similar to those found in Figure 8 (c) for example. In summary, the validation of (a) may be performed representing the simplest case.

At T >105 °C (i.e., $T > T_i$) no scattering structures can be observed. In the cooling cycle to room temperature, the generation of a highly oriented layered structure starts again at T < 90 °C with d-values decreasing from 4.80 to 4.52 nm. Below T = 66 °C, a marked orientation distribution around the substrate normal and lateral correlation peaks occur again. A quite similar behaviour

https://doi.org/10.1017/S0885715613001073 Published online by Cambridge University Press

was found for the 14 nm thin film consisting of **H10F10-54**. As expected, the scattering intensities are significantly lower. In each case, the actual layered structure in the thin films was initiated by the different temperature treatments, only. All *d*-values found in GISAXS correlate well with those of T-SAXS.

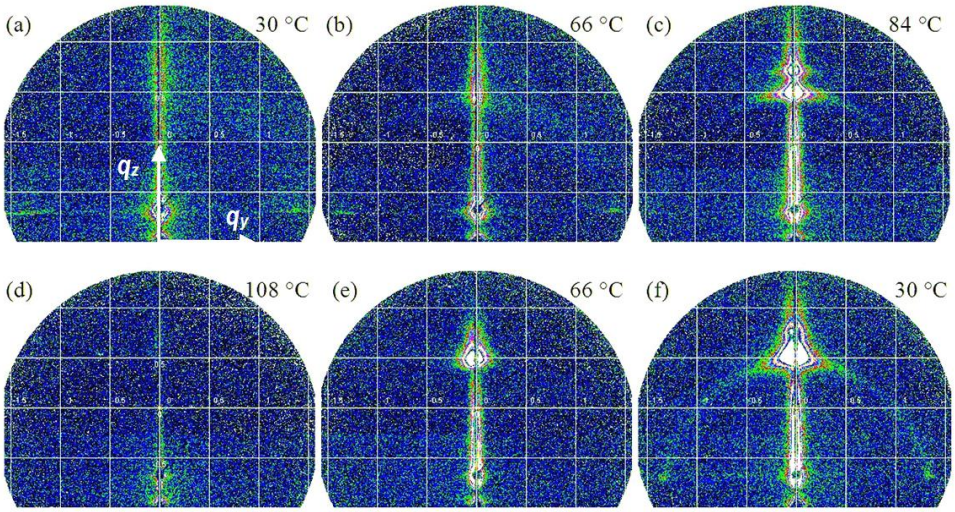


Figure 8: (Colour online) Representative GISAXS 2D patterns of sample **H10F10-36** at different temperature ((a)-(d) heating, (e)-(f) cooling). Scattering intensity plot (false colour representation) log(*I*) vs. *q* (mesh size Δq = 0.5 nm^{-1}; primary beam position: in the middle of the lower bound of the 2D GISAXS patterns, see (a)).

In contrast, thin films of the copolymers with H2F8 side chains do not show pronounced layer generation. After the temperature program, a Bragg reflection on the detector scan at d = 2.89 nm appears. The reasons for the considerably lower tendency to generate layered structures are the same as explained also for the results of XRR and GIWAXS in the subsequent annealing mode. All film data are summarized in Table III.

https://doi.org/10.1017/S0885715613001073 Published online by Cambridge University Press

TABLE III. Structure and morphology parameters from different scattering methods.

Sample		**H2F8-37**	**H2F8-72**	**H10F10-36**	**H10F10-54**
		XRR			
	Film thickness *f* (nm)	90	74	87	14
T_{ann} (°C)					
30	Layer distance *d*	--	2.68	--	(4.0) *)
50	(nm)	--	2.72	(4.1) *)	(4.0) *)
80		(2.8) *)	2.72	4.21	(4.0) *)
105		(2.8) *)	2.68	4.06	(4.0) *)
135		(2.8) *)	2.52	4.11	(4.0) *)
160		--	(not calc.)	4.06	(4.0) *)
		GIWAXS			
all T_{ann}	Mean chain distance $<d_{lat}>$ (nm)	0.547	0.537	(0.487) *)	--
T_{live} (°C)		**GISAXS**			
30	Layer distance *d*	--	--	4.72	4.7
84	(nm)	--	< 2.8 **)	4.69	4.7
105..190..90		--	--	--	--
84		--	--	4.80	4.8
66		--	2.9	4.76	4.7
30		< 2.8 **)	2.86	4.52	4.5

*) values in brackets represent very weak and/or broad structures; **) scattering maximum out of detector area

IV. CONCLUSION AND OUTLOOK

Temperature-dependant X-ray scattering methods are ideal for comparative investigations of bulk and film scattering parameters of copolymers with SF side chains and their phase separation behaviour. SAXS/WAXS bulk experiments up to 170 °C (heating/cooling cycles) were performed for basic structure information. The X-ray measurements proved formation of semifluorinated layers with *d*-spacing of 3.1 nm for P(MMA/SFMA-H2F8) and 4.4 nm for P(MMA/SFMA-H10F10) and distinct thermal extension behaviour.

As-prepared films with variable film thicknesses show very low roughness and good reproducibility. In the temperature range of side chain melting T_m the generation of layered structures starts in the case of H10F10 side chains, whereas films of H2F8 copolymers show an increasing roughness only for samples with lower SF content. Samples with higher content of SFMA-H2F8 comonomer show a layered structure, too. Temperatures higher than T_g degrade the film parameters. This tendency is stronger for copolymers with H2F8 side chains.

https://doi.org/10.1017/S0885715613001073 Published online by Cambridge University Press

Concerning the phase behaviour in bulk, the SF side chain amount and their specific fluorine content control the self-organization tendency of the semifluorinated side chains. Additionally to the structure expected from bulk behaviour, thin films are characterized by geometric confinements and orientation effects depending on the film thickness. An expansion of the existence area of layered structures could not be observed. Using GISAXS, it could be found that the spin-coated films are not in equilibrium. Only after subsequent heating an improvement of the aligned side chains perpendicularly to the film surface takes place. Also in the cooling cycle (after polymer melting and isotropization) a highly ordered/oriented structure of the film will be generated again driven by the strong incompatibility between main and side chains.

The *d*-values of the SF sublayers indicated a head-to-head arrangement of SF side chains without interdigitation and tilt in case of H2F8 side chains, whereas H10F10 copolymers show strong interdigitation of the fluorinated part of the side chains as well as a small tilt relatively to the main chain sublayer.

The behaviour found here for random copolymers is quite similar to that of diblock copolymers of PMMA and PSFMA-H2F8 with comparable composition. Random copolymers with identical side chain architectures show a weaker tendency relating the SF sublayers. Detailed X-ray scattering investigations have to be performed to clarify the effects of constrained dimensions onto a varied morphology in very thin films.

ACKNOWLEDGEMENTS

We thank all colleagues of IPF participating in synthesis and characterization of the examined copolymers. We gratefully acknowledge financial support by and participation in the former EU Network of Excellence "NANOFUN-POLY" and by the German Exchange Service (DAAD). We thank HASYLAB @ DESY Hamburg for the opportunity to carry out scattering experiments, especially the beamline operators Dr. Jan Perlich and Dr. Sergio Funari for excellent assistance.

Appelhans, D., Wang, Z.-G., Zschoche, S., Zhuang, R.-C., Häußler, L., Friedel, P., Simon, F., Jehnichen, D., Grundke, K., Eichhorn, K.-J., Komber, H. and Voit, B. (**2005**). "Bulk and surface properties of maleimide copolymers: Effect of fluorinated side chains," Macromolecules (Washington, DC, U. S.) **38**, 1655-1664.

https://doi.org/10.1017/S0885715613001073 Published online by Cambridge University Press

Busch, P. (**2003**). "Lamellare Orientierung in dünnen Diblockcopolymerfilmen – Strukturen an der Filmoberfläche und im Filminneren," PhD Thesis, Universität Leipzig (Germany).

Busch, B., Rauscher, M., Smilgies, D-M., Posselt, D. and Papadakis, C. M. (**2006**). "Grazing-incidence small-angle x-ray scattering (GISAXS) as a tool for the investigation of thin nanostructured block copolymer films - The scattering cross-section in the distorted wave Born approximation," J. Appl. Crystallogr. **39**, 433-442.

Busch, P., Krishnan, S., Paik, M., Toombes, G. E. S., Smilgies, D.-M., Gruner, S. M. and Ober, C. K. (**2007**). "Surface induced tilt propagation in thin films of semifluorinated liquid crystalline side chain block copolymers," Macromolecules (Washington, DC, U. S.) **40**, 81-89.

Friedel, P., Pospiech, D., Jehnichen, D., Bergmann, J. and Ober, C. K. (**2000**). "Polyesters with semifluorinated side chains: A proposal for the solid state structure," J. Polym. Sci., Part B: Polym. Phys. **38**, 1617-1625.

Galli, G., Martinelli, E., Chiellini, E., Ober, C. K. and Glisenti, A. (**2005**). "Low surface energy characteristics of mesophase-forming ABC and ACB triblock copolymers with fluorinated B blocks," Mol. Cryst. Liq. Cryst. **441**, 211-226.

Gopalan, P., Andruzzi, L., Li, X. and Ober, C. K. (**2002**). "Fluorinated mesogen-jacketed liquid-crystalline polymers as surface-modifying agents: Design, synthesis and characterization," Macromol. Chem. Phys. **203**, 1573–1583.

Gottwald, A., Pospiech, D., Jehnichen, D., Häußler, L., Friedel, P., Pionteck, J., Stamm, M. and Floudas, G. (**2002**). "Self-assembly and viscoelastic properties of semifluorinated polyesters," Macromol. Chem. Phys. **203**, 854-861.

Grundke, K., Pospiech, D., Kollig, W., Simon, F. and Janke, A. (**2001**). "Wetting of heterogeneous surfaces of block copolymers containing fluorinated segments," Colloid Polym. Sci. **279**, 727-735.

Höpken, J. and Möller, M. (**1992**). "Low surface energy polystyrene," Macromolecules (Washington, DC, U. S.) **25**, 1461-1467.

Jehnichen, D., Pospiech, D., Janke, A., Friedel, P., Häußler, L., Gottwald, A., Kummer, S., Kollig, W. and Grundke, K. (**2001**). "Bulk and surface structure of semifluorinated polyesters," Mater. Sci. Forum **378-381**, 378-382.

Jehnichen, D., Pospiech, D., Häußler, L., Friedel, P., Gottwald, A. and Kummer, S. (**2004**). "Self-organization in semifluorinated polymers," Mater. Sci. Forum **443-444**, 223-226.

Jehnichen, D., Pospiech, D., Häußler, L., Friedel, P., Funari, S. S. Tsuwi, J. and Kremer, F. (**2007**). "Microphase separation in semifluorinated polyesters," Z. Kristallogr. Suppl. **26**, 605-610.

Jehnichen, D., Pospiech, D., Friedel, P. and Funary, S. S. (**2011**). "Semifluorinated PMMA/PSFMA

https://doi.org/10.1017/S0885715613001073 Published online by Cambridge University Press

diblock copolymers with multiple phase separation," Z. Kristallogr. Proc. **1**, 487-492.

Li, X., Andruzzi, L., Chiellini, E., Galli, G., Ober, C. K., Hexemer, A., Kramer, E. J. and Fischer, D. A. (**2002**). "Semifluorinated aromatic side-group polystyrene-based block copolymers: Bulk structure and surface orientation studies," Macromolecules **35**, 8078-8087.

Mitchell, G. R. and Windle, A. H. (**1985**). "Diffraction from thermotropic copolyester molecules," Colloid Polym. Sci. **263**, 230-244.

Müller-Buschbaum, P. (**2003**). "Grazing incidence small-angle X-ray scattering: an advanced scattering technique for the investigation of nanostructured polymer films," Anal. Bioanal. Chem. **376**, 3–10.

Müller-Buschbaum, P. (**2009**). "A Basic Introduction to Grazing Incidence Small-Angle X-Ray Scattering," Lect. Notes Phys. **776**, 61–89.

Pospiech, D., Jehnichen, D., Gottwald, A., Häußler, L., Scheler, U., Friedel, P., Kollig, W., Ober, C. K., Li, X., Hexemer, A., Kramer, E. J. and Fischer, D. A. (**2001**). "Investigation of the microphase separation in semifluorinated polyesters," Polym. Mater. Sci. Eng. **84**, 314-315.

Pospiech, D., Komber, H., Voigt, D., Jehnichen, D., Häußler, L., Gottwald, A., Eckstein, K., Baier, A. and Grundke, K. (**2003a**). "Synthesis and characterization of semifluorinated polymers and block copolymers," Macromol. Symp. **199**, 173-186.

Pospiech, D., Jehnichen, D., Gottwald, A., Häußler, L., Kollig, W., Grundke, K., Janke, A., Schmidt, S. and Werner, C. (**2003b**). "Surface structure of fluorinated polymers and block copolymers," Surf. Coat. Int., Part B **86**, 43-52.

Pospiech, D., Häußler, L., Jehnichen, D., Kollig, W., Eckstein, K. and Grundke, K. (**2003c**). "Bulk and surface properties of blends with semifluorinated polymers and block copolymers," Macromol. Symp. **198**, 421-434.

Rauscher, M., Salditt, T. and Spohn, H. (**1995**). "Small-angle X-ray scattering under grazing incidence: the cross section in the distorded-wave Born approximation," Phys. Rev. B: Solid State **52**, 16855-16863.

Tsuwi, J., Pospiech, D., Jehnichen, D., Häußler, L. and Kremer, F. (**2007**). "Molecular dynamics in semifluorinated side-chain polysulfone studied by broadband dielectric spectroscopy," J. Appl. Polym. Sci. **105**, 201-207.

Wang, J., Mao, G., Ober, C. K. and Kramer, E. J. (**1997**). "Liquid crystalline, semifluorinated side group block copolymers with stable low energy surfaces: Synthesis, liquid crystalline structure, and critical surface tension," Macromolecules (Washington, DC, U. S.) **30**, 1906-1914.

https://doi.org/10.1017/S0885715613001073 Published online by Cambridge University Press